Biophysical Journal Volume 90 February 2006 1019–1027

Mechanically Induced Helix-Coil Transition in Biopolymer Networks

Sebastien Courty, Joanne L. Gornall, and Eugene M. Terentjev
Cavendish Laboratory, University of Cambridge, Cambridge, United Kingdom

ABSTRACT The quasi-equilibrium evolution of the helical fraction occurring in a biopolymer network (gelatin gel) under an applied stress has been investigated by observing modulation in its optical activity. Its variation with the imposed chain extension is distinctly nonmonotonic and corresponds to the transition of initially coiled strands to induced left-handed helices. The experimental results are in qualitative agreement with theoretical predictions of helices induced on chain extension. This new effect of mechanically stimulated helix-coil transition has been studied further as a function of the elastic properties of the polymer network: crosslink density and network aging.

INTRODUCTION

Biopolymer networks have been widely studied over the recent years because of their many practical applications in fields such as food, biomedical, and even photographic industries. For example, they have been extensively used for capsules, adsorbent padding, tissue regeneration and also as neutral density filters for optics. More fundamentally, biological networks (e.g., cytoskeletons with actin and microtubules) play an important role in cells by providing a structural framework which is responsible for the mechanical stability and the locomotion of the whole cell, as well as intracellular transport processes (1). Collagen networks form the core structure of bone, ligaments, and other living tissues. They have suscitated a high interest for a growing community of researchers at the interface of physics and biology (2,3).

Biopolymer networks also offer new alternatives to explore the relationship between the structure and responses at molecular length-scales. Certain homopolypeptides form regular α-helices under appropriate conditions. In this case, the molecular configurations are well understood according to the Zimm-Bragg model (4) (and its many subsequent modifications (5)). This model assumes that each segment along the polymer chain has access to only two conformational states, a random-coil state and a helical state, where the particular residue forms a hydrogen bond with other specific residues at a certain distance along the backbone. By modifying the end-to-end distance R of individual chains, the equilibrium state between the helical and the random-coil segments can evolve and a coil-to-helix transition can be induced. To determine the relationship between the helical state and the chain end-to-end distance, one needs to control the distance R and simultaneously measure the helical content. With the recent development of single-molecule force spectroscopy (SMFS), it has been possible to measure the forces generated by biopolymers and their response to applied extension forces. These experiments can tackle the question of how chiral biopolymers are held in their native state, and their pathways of folding and unfolding. Many macromolecules have been studied using SMFS including biopolymers such as DNA, xanthan, and dextran (6–8) and synthetic polymers such as poly(ethylene-glycol) (9). However, although SMFS has revealed the spectacular force-extension curves, information about the structural transitions that occur on extension of these chains (e.g., the degree of helicity in a single molecule) is difficult to obtain. Theoretical modeling of the behavior of single biopolymer molecules on extension has been hampered by this lack of access to direct information on structural changes and has only been done in specific cases.

In this article, we investigate the internal structure of a biopolymer network of helix-forming chains, and its response to an applied stress, using a new macroscopic approach combining mechanical and optical methods. We find a spectacular nonmonotonic relationship between the helical content and an externally imposed deformation, which translates to the change in end-to-end distance of network chains. In particular, we identify the effect of induced helix formation at a critical strain and further study this new effect as a function of the elastic properties of the network, using gelatin (denatured collagen) as a model system.

THEORETICAL BACKGROUND

According to the Zimm-Bragg model, each segment along a polymer chain has access to only two states: the random coil-like unbound state, and the helical state (4). The state of the polymer can therefore be described by the sequence of these units along the chain, (*hhcchcccch*...), where *h* stands for helix and *c* for coil. If the polymer, or any part of it, is in the helical state, then its effective length is shortened by a factor γ, which is $\sim$0.4 for a typical polypeptide. Since the hydrogen bonds prevent free rotation, the persistence length of the helical state is much increased compared to that of the coil, $\sim$200 nm and $\sim$1.8 nm, respectively (5,10). The number of available configurations also decreases on helix formation, and therefore the gain Δh in potential energy per

Submitted May 23, 2005, and accepted for publication October 3, 2005.

Address reprint requests to E. M. Terentjev, Tel.: 44-1223-337003; E-mail: emt1000@cam.ac.uk.

0006-3495/06/02/1019/09 $2.00

doi: 10.1529/biophysj.105.067090

monomer by forming hydrogen bonds competes with the associated loss in entropy Δs. The balance between these two forces can be expressed in terms of the free energy per monomer, $\Delta f = \Delta h - T\Delta s$, where T is the temperature. Monomers located at the ends of helical domains suffer a reduction in entropy but do not form hydrogen bonds. Therefore, monomers on the boundary between a helical and coil domain have an increased free energy of $\Delta f_t = -\Delta h$ compared to a monomer in the helical state. The effect of this term is to suppress domain boundaries; the helix-coil transition in this model is cooperative. The parameters Δf and Δf_t are usually expressed in terms of the Zimm-Bragg parameters s and σ (4),

$$s = \exp(-\beta\Delta f); \quad \sigma = \exp(-2\beta\Delta f_t), \tag{1}$$

where $\beta = 1/(k_B T)$. The factor 2 in Eq. 1 takes into account the fact that a helical domain has two boundaries with coil regions. Having identified the microscopic states of a chain, the average helical fraction of an ensemble of polymers $\langle\chi\rangle$ can be determined by the usual statistical mechanics calculation maximizing the partition function,

$$Z = \sum_{s_1 s_2 \ldots s_N} e^{-\beta F([s_1 s_2 \ldots s_N])}, \tag{2}$$

where s_i is either c or h and the sum is performed over all possible states of the variables s_i, $i = 1 \ldots N$. The total free energy F, which depends on (s_i), is the sum of the monomer free energies given by Δf and Δf_t. This procedure gives a higher statistical weight to configurations with a large number of small domains rather than a small number of large domains; for a fixed number of helical domains there are more possible rearrangements that can occur without a change in energy (provided helix still follows coil and vice versa) for a large number of small domains.

Recently, Tamashiro and Pincus (11), and Buhot and Halperin (12) have shown that by imposing an extension on such a helix-forming chain, which is kept above but close to the spontaneous helix-coil transition, one can stimulate the helical state (which corresponds to a natural enthalpy well Δh) by reducing the randomizing effect of chain entropy ($\Delta s < 0$) due to the stretching of its ends. The problem can be simplified by neglecting the mixing entropy without changing the outcome qualitatively, and only slightly quantitatively, i.e., assuming the helical and coil domains are separated into two blocks with a fixed interface energy Δf_t, Fig. 1. The free energy of the chain in this case is then given by

$$F_{ch} = \chi N\Delta f + 2\Delta f_t + \frac{3(R - \gamma a N\chi)^2}{2(1-\chi)Na^2}, \tag{3}$$

where $\Delta f = \Delta h - T\Delta s > 0$ and N is the total number of monomers of length a. The first two terms give the free energy of a helix, with its interface, and they are positive since under our assumption the chain is above its spontaneous coil-helix transition. The last term represents the Gaussian entropic free energy describing the coil fraction with an end-to-end distance R minus the distance bridged by the helical part of the chain, with the reduced contour length available to the coil. Here $\chi \in (0, 1)$ is the helical content and γ the geometric factor accounting for the helix length, per monomer. Depending on parameters, this model predicts that the helical content of the chain, $\chi(R)$, may increase on stretching (with or without a threshold), finding an optimal balance between the two competing factors increasing the total F_{ch}. Eventually all the chain is in the α-helix ($\chi = 1$) and on further extension, one would of course force the helix to unwind.

This model of a single helix-forming polypeptide was later extended to predict the stimulated helix-coil transition occurring in a cross-linked random network of such chains under external deformation (13). Within a basic network theory, assuming the affine deformation of random strands through their endpoints and performing the quenched average over the network topology, the average helical content (per chain) is given by

$$\langle\chi\rangle(\underline{\underline{\boldsymbol{\lambda}}}) = \int d\mathbf{R}\chi(|\underline{\underline{\boldsymbol{\lambda}}}\,\mathbf{R}|)P(\mathbf{R}), \tag{4}$$

where $\underline{\underline{\boldsymbol{\lambda}}}$ is the affine volume-conserving strain tensor and the quenched probability distribution of finding a network strand with a given number of monomers N, and end-to-end distance at formation $\boldsymbol{R}$ is given by $P(R) \propto \exp(-F_{ch}(R)/k_B T)$. In a random network, depending on their orientation, some strands are extended and some are compressed; the average helical content $\langle\chi\rangle$, however, remains a nonmonotonic function of uniaxial extension as long as the chains are slightly denatured (above but close to their natural helix-coil transition: Δf positive but small). Fig. 2 shows an example of this model's predictions for the specific case of uniaxial extension of the sample by a factor λ. It can be seen that the average helical content in the network increases on uniaxial extension (as well as on compression, due to incompressibility) and goes through a maximum at a certain λ.

EXPERIMENTAL METHODS

We used gelatin networks as a model system. Gelatin gels are good candidates for such experiments, as their constituting chains are mostly in the denatured (coil) state and the samples can be stretched with their optical activity simultaneously measured. Moreover, gelatin gels are well described in the literature (14) and are by far the most studied functional biopolymer due to its extensive practical use. The gelatin network is held together by

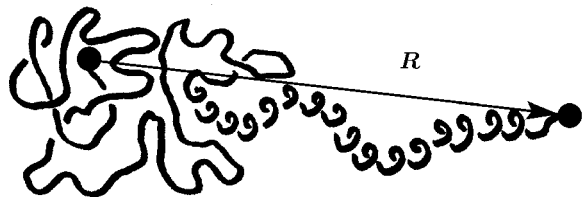

FIGURE 1 The sketch of the chain with helical and coil fractions, at constrained end-to-end distance R.

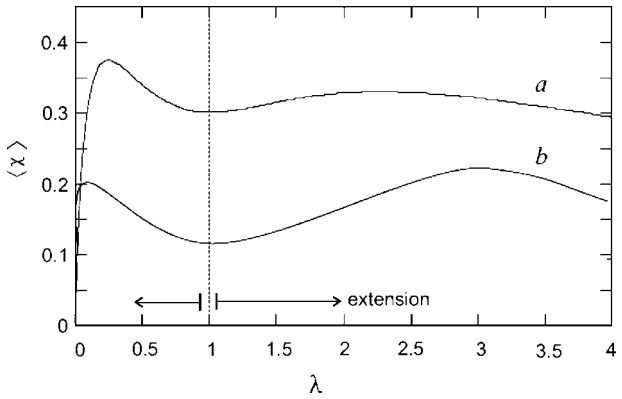

FIGURE 2 The mean helical fraction of a network stretched by a factor λ, according to Li et al. (7) for $N = 100$ and $\beta\Delta f = 0.05$ (curve *a*), $\beta\Delta f = 0.1$ (curve *b*, for chains further away from the helix-coil transition).

effective crosslinks made of right-handed (tertiary) superhelices stabilized by hydrogen bonds, resulting from the wrapping of three left-handed helical segments of otherwise denatured collagen chains.

Sample preparation

Gelatin samples were prepared by dissolving gelatin powder (from Sigma, St. Louis, MO) in ethylene glycol. The main reason for using ethylene glycol instead of more traditional water is to allow us to conduct experiments over long periods of time and not worry about solvent evaporation (boiling point $T_B \approx 190°$). As we indicate below, there are good reasons to believe that the intrinsic chain responses are qualitatively the same in ethylene glycol, although the specific magnitudes of elastic modulus and helix content at any given temperature may be slightly different. Fig. 3 shows the percentage change in the mass of gelatin gel in ethylene glycol. As the gel consolidates, its mass increases initially (presumably due to equilibrium hydration in the atmosphere) and then shows a weak linear decrease. The rate of this decrease is slow enough on the timescale of our experiments (typically 30 min) to have no significant effect on our results.

The sol-gel transitions of water and ethylene glycol (EG) gels have been investigated using differential scanning calorimetry (DSC), using a Perkin-Elmer Pyris 1 calorimeter (Boston, MA). The gels, kept in air-tight aluminum pans, were heated at a rate of 5°C/min from 20 to 65°C. The melting point, T_m, of the gel was determined from the peak of the DSC endotherm. Fig. 4 shows T_m as a function of concentration for water and ethylene glycol

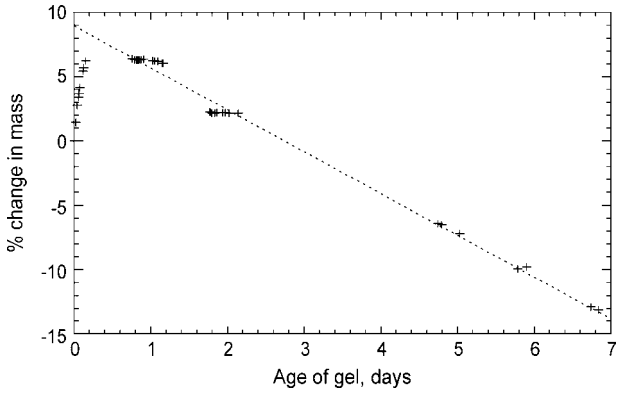

FIGURE 3 Mass change an ethylene glycol gelatin gel at room temperature in the air. The mass rises initially, then shows a linear decrease at a slow rate of ~3.3% per day.

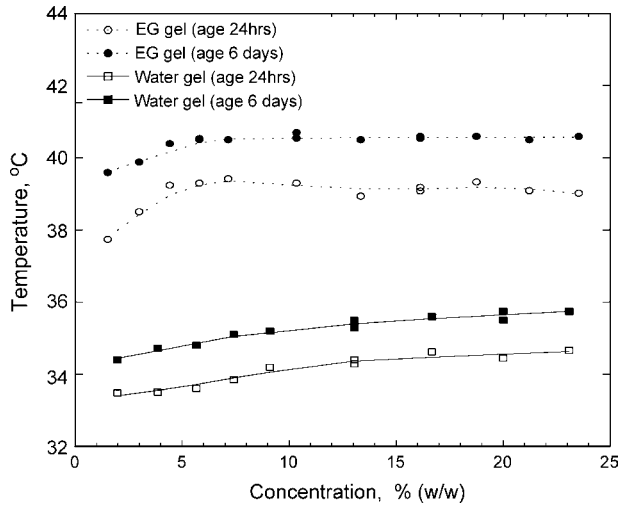

FIGURE 4 Melting point, T_m, as a function of concentration, obtained from DSC, for ethylene glycol (*EG*) and water gelatin gels aged at room temperature for 24 h and six days. Respective curves are labeled on the plot.

gels, aged at room temperature for one day and six days after the initial mixing. The melting temperature increases as the gel ages and is ~5°C higher for ethylene glycol gels, compared to water gels.

Fig. 5 shows that the increase in the transition enthalpy for the whole sample, ΔH, with polymer concentration is almost perfectly linear and is roughly the same for water and ethylene glycol gels aged for one day for concentrations below 24% (w/w), and for gels six-days-old below 10% (w/w). Above this concentration, the enthalpy change is slightly greater for water gels.

Assuming the increased transition temperatures seen in ethylene glycol gels are simply due to the greater viscosity of EG (with finite rate of temperature change in the DSC), the density of the crosslinks formed by the gelatin molecules in water and ethylene glycol gels could be very similar. To determine the effect of gelatin concentration, stretching experiments were performed using 12% and 16% (w/w) EG gels.

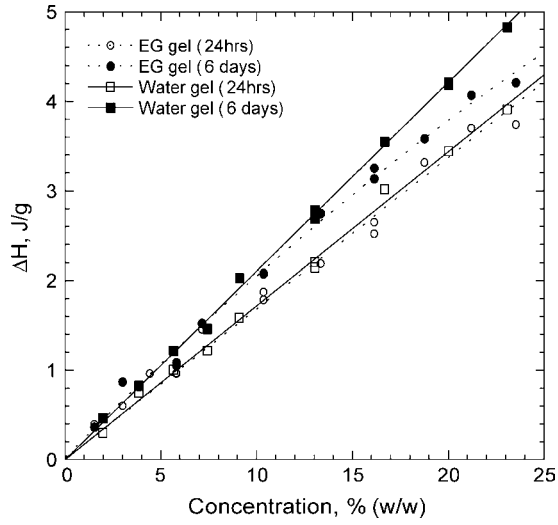

FIGURE 5 Transition enthalpy, ΔH, as a function of concentration, obtained from DSC for ethylene glycol (*EG*) and water gels aged at room temperature for 24 h and six days. Respective curves are labeled on the plot.

One important point about sample reproducibility has to be made. Collagen from different sources, as well as samples prepared in different batches, always differ in their properties. We did not specifically undertake a task of making all samples uniformly comparable. All reported effects are qualitatively reproduced; however, small quantitative differences would always be observed. Naturally, when samples had to be quantitatively compared (such as in aging, or crosslinking density analysis), they were always prepared from the same batch and at the same time.

The mixture was kept above the gel transition point at 65°C under continuous stirring to ensure homogeneity and consistent thermo-mechanical history of each experiment. After cooling down to room temperature each time, a cross-linked gel sheet of dimension $1.5 \times 7 \times 20$ mm was prepared. The mechanical properties of the gelatin quenched below its gel point have been investigated using a Dynamic Stress Rheometer (Rheometrics, Piscataway, NJ). Fig. 6 shows the variation in linear storage modulus, G', over 10 days after quenching the 16% EG gel to room temperature. The modulus rises initially when the elastic network is held together by the triple-helix crosslinks, reaching a constant value of 1.7×10^4 Pa after four days. At this point, we assume the crosslinking is completed (leaving aside delicate issues of slow drift of collagen toward its natural state, irrelevant on our timescales). To determine the effect of the variation in G' on the optical rotation, stretching experiments were performed one day after the gel was removed from the mold, when the storage modulus was still rising, and after six days, when G' had reached equilibrium; both aging points are marked on the plot.

Opto-mechanical apparatus

The opto-mechanical experiments have been carried out by combining a dynamical method for measuring the optical rotation Ψ and a stress-strain apparatus, Fig. 7. Gelatin networks, typically of dimension $1.5 \times 7 \times 20$ mm, were mounted using clamps between a temperature-compensated force transducer (Pioden Controls, Canterbury, UK) and a micrometer screw gauge controlled by a stepper motor. The force transducer allowed for measurements of stress $\sigma = f(\lambda)$ as the sample was strained along the λ_{xx} axis. Samples were stretched at a strain rate of 0.001 s^{-1}. Simultaneously, we measured the optical rotation Ψ of the gelatin gel with a linearly polarized light at 633 nm from a He-Ne laser. The reason for choosing this long wavelength is to stay away from any molecular absorption band characteristic of circular dichroism (CD). That method of detecting protein (and other) helices is totally inappropriate for our study because the interpretation of CD signal is notoriously ambiguous. Any distortions of the helices, such as bending, can have a significant affect on the CD spectrum. It would certainly be inapplicable in our case when the helices are distorted by the network deformations. Our method of choice is the optical rotation of plane-polarized light in nonabsorbing region, which can be demonstrated to be linearly proportional to the concentration of helically correlated regions of chains.

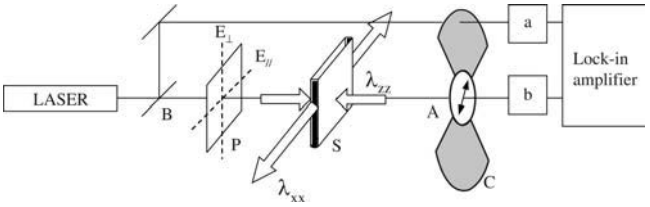

FIGURE 7 Scheme of the apparatus which combined optical rotation rate $\partial\Psi/\partial z$ and stress-strain $\sigma = f(\lambda)$ measurements. The components are: (*B*) beam splitter; (*P*) polarizer; (*S*) sample mounted, using clamps, between a temperature-compensated force transducer and micrometer screw gauge controlled by a stepper motor (not shown); (*A*) analyzer; and (*C*) light chopper rotating on the same frame as *A*.

As shown in Fig. 7, the laser beam is split into two parts, one plane-polarized beam (labeled *b* in Fig. 7) passing through the sample and an analyzer, rotating at a fixed frequency ~16 Hz, the other (beam *a*) through an optical chopper mounted on the same rotor and providing a reference signal. The lock-in amplifier (Stanford Research, Menlo Park, CA) locked on the reference signal and detected the relative phase difference $\Delta\Theta$ between the two signals. The phase shift corresponds to the rotation of the plane of the linearly polarized light and gives directly the total rotation angle Ψ. The helix content is a material function proportional to the rate of optical rotation $\partial\Psi/\partial z$, so we need to take into account the change of path length of light d (along z, the sample thickness) as a function of the imposed uniaxial extension $\lambda = \lambda_{xx}$. If we model the deformation as strictly volume-conserving, then $\det(\underline{\lambda}) = \lambda_{xx}\lambda_{yy}\lambda_{zz} = 1$. If the deformation is also isotropic, $\lambda_{yy} = \lambda_{zz}$ and we expect $\lambda_{zz} = 1/\sqrt{\lambda_{xx}}$. To verify this, the width of a sample was measured using a traveling microscope as a function of λ_{xx}. Fig. 8 shows that, on stretching the gel, λ_{zz} and λ_{xx} accurately satisfy the predicted $(1/\sqrt{\lambda})$ relation and hence the measured raw optical rotation of a sample was corrected to give the rate of optical rotation $\partial\Psi/\partial z \propto \Psi\sqrt{\lambda}$. The measured stress was also corrected for the corresponding decrease in the cross-sectional area (in the y,z plane) on stretching. Then the true stress, σ', is related to the measured nominal stress by $\sigma' = \lambda\ \sigma$.

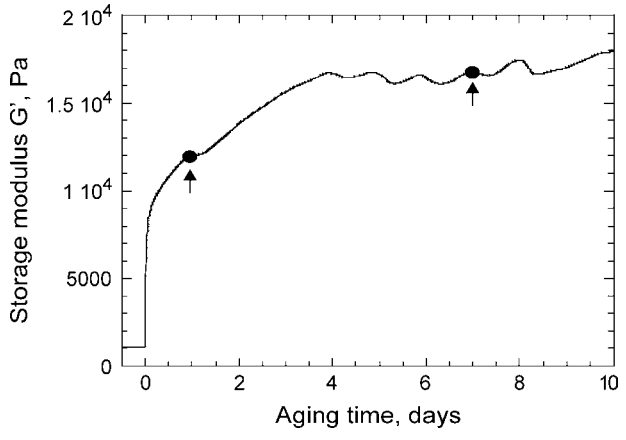

FIGURE 6 Variation of the storage modulus G' with time after quenching the 16% EG gel to room temperature (at $t = 0$ point). G' rises over four days to reach an equilibrium value of 1.7×10^4 Pa. Arrows point at the two aging states at which main experiments have been performed (see text).

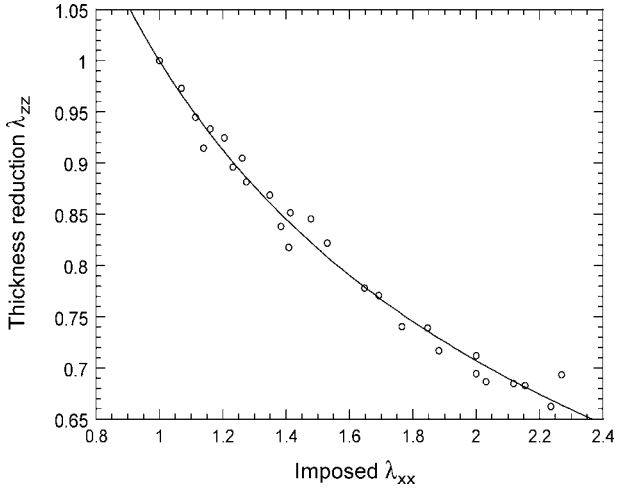

FIGURE 8 Variation of λ_{zz} with λ_{xx}. The curve corresponds to the transversely isotropic incompressible $\lambda_{zz} = 1/\sqrt{\lambda_{xx}}$.

Effect of induced birefringence

The changes in rotation may be affected by birefringence, which is necessarily induced in the network on uniaxial stretching. The gel is initially isotropic, but on extension, the statistical distribution of the polymer becomes biased. This is a very well-known effect observed in any polymer network under uniaxial deformation. The induced birefringence is defined as $\Delta n = n_{SD} - n_{ND}$, where n_{SD} and n_{ND} are the refractive indices in the stretching and the normal directions. In our case, this effect was measured separately with the aid of a quarter-wave plate inserted in the beam-path of our apparatus, using a method based on the phase differences of coherent light, and one which is therefore insensitive to intensity changes due to, for example, scattering. Fig. 9 shows the induced birefringence, Δn, which is almost a linear function of imposed extension λ_{xx}, for a 16% gelatin sample. It can be shown (15) that the induced birefringence is proportional to the difference in the normal stress, $\Delta n = C(\sigma_{zz} - \sigma_{xx})$, with C the so-called stress optical coefficient, which depends only on the local structure of the polymer. For our gelatin gel, we determine $C \approx 1.6 \times 10^{-6}$ cm^2/N, which agrees well with the literature data on a variety of polymer networks, from dry rubber to highly swollen gels (16,17).

One could in principle observe a rotation of the plane of polarization, related to the induced birefringence Δn, if the initial light polarization falls on the sample at an oblique angle to the extension axis. The corresponding rotation angle is $\theta \sim \pi \Delta n \lambda_{zz} d/\Lambda$, where Λ is the laser wavelength and d the sample thickness. At our highest extension and other parameters, we may obtain the value $\theta_{max} \sim 6°$. We shall see that this value is almost an order-of-magnitude below our readings. However, there is a second factor making the effect of induced birefringence irrelevant. In our case, we deliberately send the incident light with polarization aligned with the axes of deformation. If the sample was not optically active, there would be no rotation at all. As the plane of polarization starts its rotation away from this initial position, as the light travels along its path, the effects of birefringence kick in. The birefringence simultaneously induced in the sample acts to rotate the plane of polarization back toward the axes of deformation. That would reduce the amplitude of the perceived optical rotation, by the amount significantly less than θ_{max}. As the main effect described in this article is a dramatic increase in the magnitude of optical rotation on stretching, we conclude that the induced birefringence has little effect.

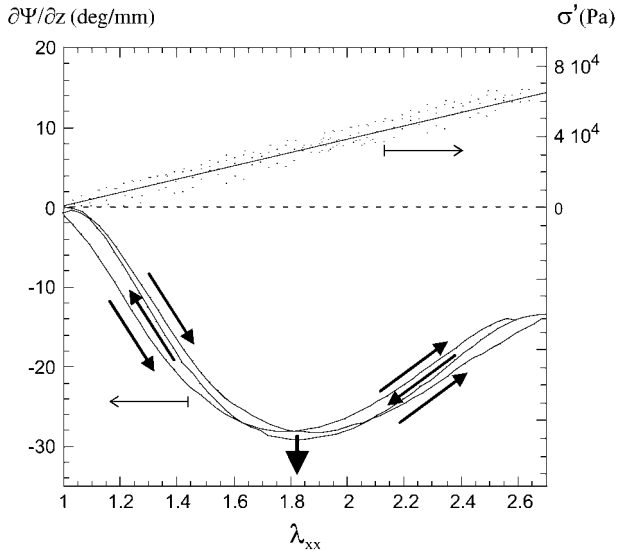

FIGURE 9 Evolution of the rotation rate $\partial\Psi/\partial z$ (*left axis*) and stress σ' (*right axis*) as functions of imposed λ_{xx}, for a 16% gel. The plot shows the data of the extension, retraction, and second extension cycles of the sample, to demonstrate the reversible equilibrium nature of the response.

RESULTS AND DISCUSSION

The equilibrium content of secondary helices in a crosslinked gel changes as a function of the applied stress. By combining dynamic-mechanical and optical measurements, Fig. 10 shows the changes in optical rotation rate, $\partial\Psi/\partial z$, which are a direct measure of the helical content, as a function of imposed extension λ_{xx}. This result, generic to this gelatin system (i.e., reproducing qualitatively over a wide range of concentrations and temperatures), demonstrates that by imposing an extension on chains, one can stimulate the helix formation in the network strands.

The initial optical rotation of the unstretched network is negative, $\partial\Psi/\partial z(\lambda = 1) \approx -0.63°$/mm, which in our setup corresponds to left-handed rotation. The optical rotation of a gelatin solution at this concentration, at 50°C, when the chains are in the random coil state, is an order-of-magnitude smaller ($\approx -0.06°$/mm) and still left-handed. The optical rotation response of native collagen has been compared to that of synthetic peptides such as poly-proline. In aqueous solution, proline polypeptides adopt the poly-L-proline II conformation, which is a single left-handed helix, almost identical to the collagen left-handed secondary helix (18). The optical rotation of poly-L-proline II solutions shows similar behavior to that observed for native collagen solutions (19). The association of the helices to form the tertiary triple helix marginally distorts the helical folded regions of chains, but has little effect on the rotatory properties. The optical rotation measurement is, therefore, mainly sensitive to the left-handed secondary helical structure of individual chains. The small negative rotation measured initially (in the undistorted gelatin sample, $\lambda = 1$) is due to these secondary α-helices, which are joined into triple-helical regions that form the crosslinks in the gel. Some additional single helices may be present as well, but cannot be distinguished from those forming the triple helices.

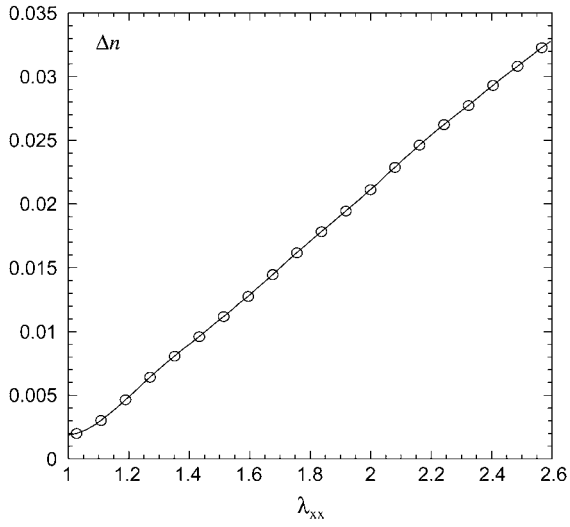

FIGURE 10 Birefringence, Δn, as a function of imposed λ_{xx}, for a 16% gel.

On extension, the absolute value of the rotation rate increases dramatically. At the same time, over the large range of extensions λ_{xx}, the stress-strain relationship remains strictly linear and fully reversible. From this, we may infer that the total amount of network crosslinks (right-handed triple-helix regions) remains constant over the duration of this experiment and the nonmonotonic variation of optical rotation with extension is not due to structural changes of the triple helical crosslinks. The dramatic increase of the optical activity suggests an increase of left-handed single-strand α-helix population. These helices are generated in the originally coiled network strands and produce the increasing left-handed rotation (represented as negative values of rotation rate in Fig. 10).

At higher extension, λ_{xx}, the variation of the optical rotation is clearly nonmonotonic and we found a maximum value of its amplitude $-28.8°$/mm for $\lambda^* \approx 1.85$, as shown by the arrow in Fig. 10. We assume this corresponds to the maximum content of helices in the network, which subsequently start to unwind for strain $\lambda > 2$. This crossover is a consequence of the change in the nature of the helix coil transition which becomes a helix-extended coil transition for strong forces (20). The minimum in the optical rotation could reflect the point at which the rotation due to the induced birefringence dominates that resulting from the formation of helices, leading to an increase in the optical rotation. However, as the magnitude of the rotation due to birefringence is small compared to the measured rotation, even at our highest extension, it is likely that the result of the birefringence is to shift the measured critical extension to a somewhat smaller value than the true extension at which the helices begin to unwind.

Our interpretation of the nonmonotonic left-handed rotation depends on the assumption that the conformation of the triple helical crosslinks in the network is preserved; this is illustrated by performing a repeated stretching-contracting cycle experiment. In Fig. 10, only an insignificant hysteresis is observed. This, and the consistently linear stress-strain variation, suggests that the change in average helical content on stretching is not due to topological rearrangement of triple-helical junction zones (even though a decrease of their density in the network could have been initially suspected). To test the equilibrium in a different way, an unstretched sample was extended very rapidly to $\lambda = 1.2$. The optical rotation and stress were then measured over several hours (Fig. 11). It is quite clear that the effects observed while stretching the sample at a slow rate of 10^{-3} s^{-1} are close to equilibrium.

We therefore conclude that the imposed strain promotes the induced helix-coil transition on originally randomly coiled collagen segments of the elastic network, which results in a large and nonmonotonic variation of the overall optical activity.

Influence of crosslinks density

The influence of the network properties on the stimulated helix-coil transition has been studied by measuring the

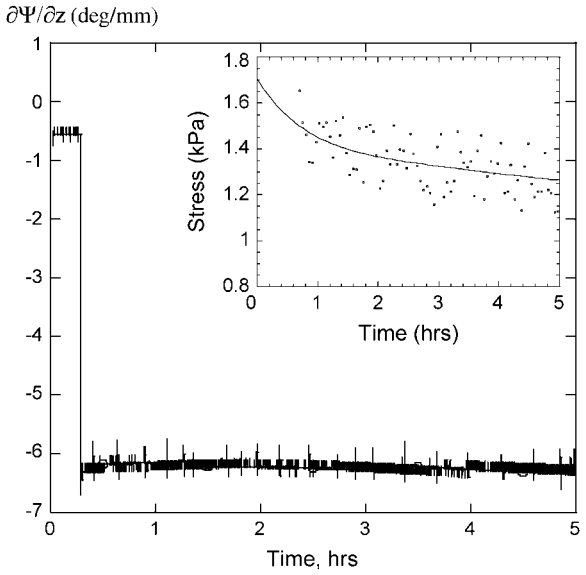

FIGURE 11 Time evolution of rotation rate after a strain step of ~20%, illustrating the stability of the microstructure. The inset shows the corresponding slow stress relaxation, which is a well-known feature of any rubbery network.

generic response described above as a function of the crosslink density. The crosslink density at a fixed temperature is directly related to the concentration of gelatin and two different samples have been prepared with 12% and 16% of gelatin (w/w). Fig. 12 shows the results of stretching experiments performed on a 12% (w/w) and a 16% (w/w) gelatin gel (aged for six days after quenching, when the storage modulus G' had reached equilibrium; see Fig. 6). The rates of optical rotation $\partial\Psi/\partial z$ of unstretched (at $\lambda_{xx} = 1$) 12% and 16% samples are $-0.40°$/mm and $-0.63°$/mm, respectively. This is consistent with the expectation that fewer triple-helical crosslinks will form in a 12% gel. On stretching, the variations in optical rotation for both 12% and 16% gelatin gels are nonmonotonic with the imposed deformation λ_{xx}. However, a difference is observed on the magnitude of $\partial\Psi/\partial z$, whereas the critical strain, $\lambda^* \approx 1.85$ is similar for both samples. For a 12% gel, the rotation rate reaches a maximum value of $\sim -18°$/mm, smaller than the value of $\partial\Psi/\partial z = -46.4°$/mm for the 16% gel. On the corresponding stress-strain curves, we find the consistently linear increase with the extension λ_{xx}, but the value of extension (Young) modulus E for a 12% gelatin gel is approximately one-third of those for a 16% gel, again consistent with the expected reduction in the number of crosslinks.

Influence of network aging

We examined how the gelatin aging influences the mechanically stimulated helix generation in the network. For this purpose, experiments have been performed as a function of the storage modulus G' evolution: after one day from gel

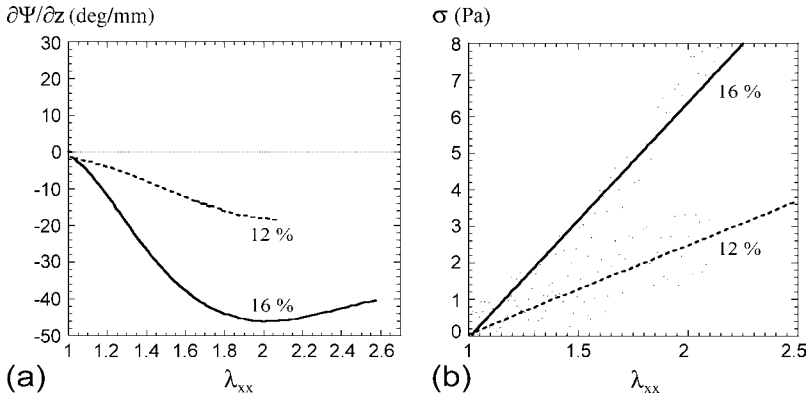

FIGURE 12 (*a*) Variation of the optical activity $\partial\Psi/\partial z$ for 12% and 16% gels on stretching, six days after the gels were removed from the mold. (*b*) The corresponding stress-strain measurements.

quenching when G' is still rising, and after six days when G' reaches a plateau (constant value of 1.7×10^4 Pa), from which we assume that the equilibrium crosslinking is completed. The results are presented in Fig. 13, which shows the variation of $\partial\Psi/\partial z$ as a function of λ_{xx} for a 16% gelatin gel after one day and six days of aging from quenching. For a one-day-old gel, the initial optical rotation for the unstretched sample is $\partial\Psi/\partial z = -0.58°$/mm for the 16% gel and $-0.38°$/mm for the 12% gel. This is smaller but close to the optical activity of a six-day-old gel, at each concentration, which is consistent with their similar extension modulus values. In both cases, on the corresponding stress-strain curves, we find a linear relationship as shown on Fig. 13 *b*. The values of the Young modulus E (by assuming the Poisson's ratio $r = 0.5$), calculated from the stress-strain relation in Fig. 13, compare favorably with those obtained using the dynamic rheometer: one expects, and indeed finds $E \approx 3G'$. As the gel ages, the helical content increases and the network becomes stiffer. This is a result of the lengthening of the right-handed triple helices, reported and discussed in, e.g., Guo et al. (21).

On stretching, the rate of optical rotation for a one-day-old gel becomes negative and shows the same characteristic nonmonotonic variation. However, the value of the optical activity at the critical strain λ^* is much lower than the value obtained for a six-day old gel: for instance, for the 16% gel the maximum values of right-handed rotation rate are $\partial\Psi/\partial z = (-12.0 \pm 0.5)°$/mm and $\partial\Psi/\partial z = (-46.4 \pm 0.5)°$/mm, respectively. This, with the results obtained as a function of cross-links density, confirms that the induced helical content depends strongly on the elastic properties of the network, which has to transmit deformation to individual collagen strands to induce their helices.

Optical anisotropy of induced helices

We have further investigated the uniaxial anisotropy of induced helices with sending the light through the stretched sample, which was polarized perpendicular (electrical field $E \perp \lambda_{xx}$) and parallel ($E \| \lambda_{xx}$) to the direction of extension. The results for a six-day-old 16% gel are shown in Fig. 14.

For the light that is initially polarized perpendicular to the direction of extension, the rate of optical rotation is consistently greater than that obtained when the polarization plane is initially parallel to λ_{xx}. The difference between the rotation rates in these parallel and perpendicular geometries increases as the strain is increased up to the critical strain. Qualitatively similar results are obtained for 12% gels and for one-day-old gels. This effect is a signature of an optical anisotropy of induced helices.

The peptide bond is optically anisotropic on itself ($\Delta\alpha_0 = 2 \times 10^{-30}$ m^3) (22). When amino acids are arranged in

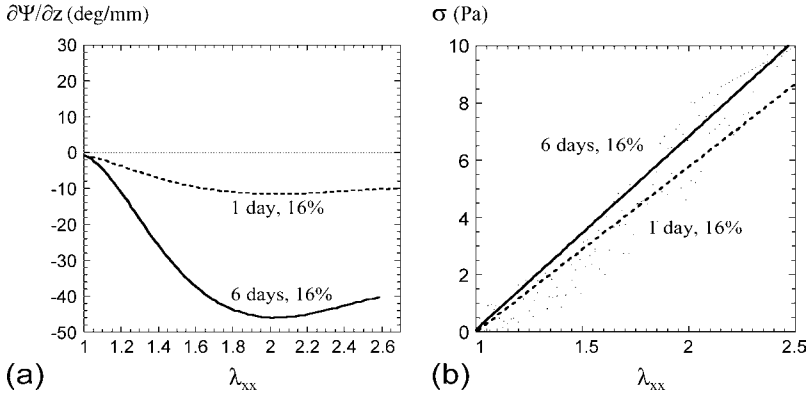

FIGURE 13 (*a*) Variation of the optical activity $\partial\Psi/\partial z$ for a one-day- and a six-day-aged 16% gel. (*b*) The corresponding stress-strain measurements showing only minor variation in the modulus.

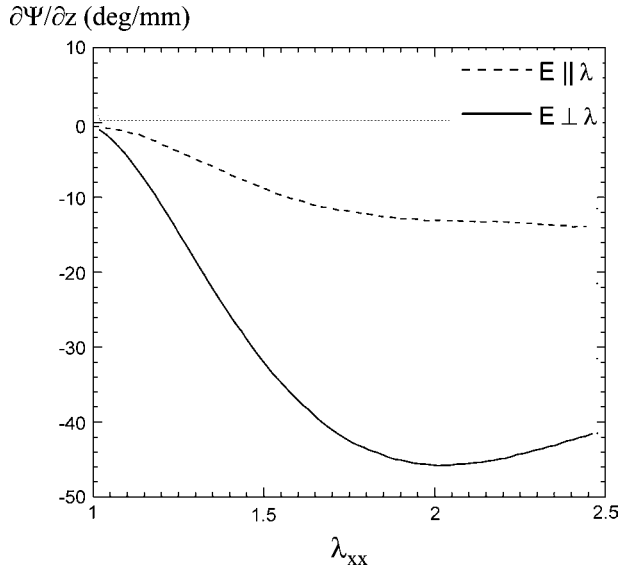

FIGURE 14 The optical activity $\partial\Psi/\partial z$ for a six-day-aged 16% gel, sampled with the light, which is linearly polarized parallel and perpendicular to the axis of uniaxial stretching.

a straight α-helix, the average uniaxial anisotropy along the helical axis is clearly induced (also known as the transversely isotropic symmetry of the local dielectric tensor). Assuming the helix is a relatively rigid structure, at least in comparison with the coil chain regions, one expects their alignment induced by the uniaxial strain applied to the system. This alignment of an induced helix along the force axis is also a feature of the original models of individual chains (11,12). A simple affine model calculating the average uniaxial anisotropy induced in the orientational distribution of rigid rods embedded in an elastic continuum, which is uniaxially stretched by a factor λ, predicts the distribution function

$$P(\theta) = \frac{\lambda^3}{2(\cos^2\theta + \lambda^3\sin^2\theta)^{3/2}}\sin\theta d\theta, \qquad (5)$$

with θ the local angle of a helix axis to the direction of strain. This has to be multiplied by the (yet unknown) factor of anisotropy of helix polarizability, and then convoluted with the nonmonotonic function describing the helix concentration; see Fig. 2 and Theoretical Background, above, to account for the observed effect of light polarization.

CONCLUSIONS

We performed a numerical integration similar to that of Kutter and Terentjev (13) to obtain the effective optical rotation rate, by weighting the (scalar) helical fraction by the orientational bias of incident light polarization with respect to the applied deformation. As would be expected, for a fixed helical fraction, the rotation rate is greater for the light that is initially polarized perpendicular to the helix axis, suggesting the negative dielectric anisotropy. We applied this model to the gelatin network used in this investigation. The value of the parameter N, the average number of chain segments between crosslinks, is not straightforward to estimate, as the effective crosslinks do not form at the ends of the molecule. The distance between crosslinks ξ could be estimated from the measured shear modulus, $G \approx (k_BT/\xi^3)$, assuming basic rubber elasticity response. For a 16% six-days-old gelatin gel, this gives $\xi \sim 6 \times 10^{-9}$ m. Since the dimensions of an amino acid are of the order of a few Ångströms, this suggests $N \sim 100$ for the gelatin network. To fit the position of the rotation rate maximum, we required the parameter $\beta\Delta f = 0.05$, at $N = 100$ (see Theoretical Background, above). Assuming the optical rotation linearly increases with increasing helical content, this model shows qualitatively the same variation with extension as the results obtained with the gelatin gel.

In summary, the structural changes occurring in a biopolymer network (gelatin gel) on extension have been monitored by observing changes in its optical activity. We have demonstrated experimentally the mechanical induced helix-coil transition by applying an external deformation (imposed end-to-end distance) of the network. The initially small negative rotation of the plane of polarization by the gel, due to the right-handed triple helical crosslinks, becomes large on stretching and shows a distinct nonmonotonic variation with the imposed strain. This nonlinear variation is not due to birefringence and depends strongly on the elastic properties of the network. This result, in qualitative agreement with theoretical predictions for $\beta\Delta f = 0.05$ and $N = 100$, gives a consistent picture of induced helix-coil transition occurring in polymer networks under stress. However, the dependence of the observed changes in optical rotation on the plane of polarization remains to be explained.

Discussions with R. Colby, A. Craig, S. Kutter, and the help of K. Lim with many of the measurements, are gratefully appreciated.

We thank Engineering and Physical Sciences Research Council for financial support.

REFERENCES

1. Boal, D. 2002. Mechanics of the Cell. Cambridge University Press, Cambridge, UK.
2. MacKintosh, F. C., J. Käs, and P. A. Janmey. 1995. Elasticity of semiflexible biopolymer networks. *Phys. Rev. Lett.* 75:4425–4428.
3. Gisler, T., and D. A. Weitz. 1999. Scaling of the microrheology of semidilute F-actin solutions. *Phys. Rev. Lett.* 82:1606–1609.
4. Zimm, B. H., and J. K. Bragg. 1959. Theory of the phase transition between helix and random coil. *J. Chem. Phys.* 11:526–535.
5. Grosberg, A. Y., and A. R. Khokhlov. 1994. Statistical Physics of Macromolecules. AIP Press, New York.
6. Perkins, T. T., S. R. Quake, D. E. Smith, and S. Chu. 1994. Relaxation of a single DNA molecule observed by optical microscopy. *Science.* 264:822–826.

7. Li, H., M. Rief, F. Oesterhelt, and H. E. Gaub. 1998. Single-molecule force spectroscopy on xanthan by AFM. *Adv. Mater.* 3:316–319.
8. Rief, M., F. Oesterhelt, B. Heymann, and H. E. Gaub. 1997. Single-molecule force spectroscopy on polysaccharides by atomic force microscopy. *Science.* 275:1295–1297.
9. Rief, M., J. M. Fernandez, and H. E. Gaub. 1998. Elastically coupled two-level systems as a model for biopolymer extensibility. *Phys. Rev. Lett.* 81:4764–4767.
10. Poland, D., and H. A. Scheraga. 1970. Theory of Helix-Coil Transitions in Biopolymers. Academic Press, New York.
11. Tamashiro, M. N., and P. Pincus. 2001. Helix-coil transition in homopolypeptides under stretching. *Phys. Rev. E.* 63:021909.
12. Buhot, A., and A. Halperin. 2002. Extension behavior of helicogenic polypeptides. *Macromolecules.* 35:3238–3252.
13. Kutter, S., and E. M. Terentjev. 2002. Networks of helix-forming polymers. *Eur. Phys. J. E.* 8:539–546.
14. Joly-Duhamel, C., D. Hellio, and M. Djabourov. 2002. All gelatin networks. I. Biodiversity and physical chemistry. *Langmuir.* 18:7208–7217.
15. Doi, M., and S. F. Edwards. 1986. The Theory of Polymer Dynamics. Oxford University Press, Oxford, UK.
16. Rennar, N. 1998. Birefringence and rubber-elastic properties of cross-linked polymers in uniaxial deformation. *Phys. Chem. Chem. Phys.* 102:1665–1671.
17. Hahn, O., and D. Woermann. 1997. Strain-birefringence of a polyelectrolyte gel. *Phys. Chem. Chem. Phys.* 101:703–707.
18. Djabourov, M., J. Leblond, and P. Papon. 1988. Gelation of aqueous gelatin solutions. I. Structural investigation. *J. Phys. France.* 49:319–332.
19. Blout, E. R., J. P. Carver, and J. Gross. 1963. Intrinsic cotton effects in collagen and poly-L-proline. *J. Am. Chem. Soc.* 85:644–651.
20. Varshney, V., and G. A. Carri. 2005. Stretching helical semiflexible polymers. *Macromolecules.* 38:780–787.
21. Guo, L., R. H. Colby, and A. M. Howe. 2003. Physical gelation of gelatin studied with rheo-optics. *Macromolecules.* 36:10009–10020.
22. Bras, W., G. P. Diakun, J. F. Diaz, G. Maret, H. Kramer, J. Bordas, and F. J. Medrano. 1998. The susceptibility of pure tubulin to high magnetic fields: a magnetic birefringence and x-ray fiber diffraction study. *Biophys. J.* 74:1509–1521.